Reciprocal Damon-Eshbach-type spin wave excitation in a magnonic crystal due to tunable magnetic symmetry

R. Huber,[1] M. Krawczyk,[2] T. Schwarze,[1] H. Yu,[1] G. Duerr,[1] S. Albert,[1] and D. Grundler[1,a]

[1]*Lehrstuhl für Physik funktionaler Schichtsysteme, Technische Universität München, Physik Department, James-Franck-Str. 1, D-85747 Garching b. München, Germany*
[2]*Faculty of Physics, Adam Mickiewicz University, Umultowska 85, Poznań 61-614, Poland*

We report spin-wave (SW) propagation in a one-dimensional magnonic crystal (MC) explored by all electrical spectroscopy. The MC consists of a periodic array of 255 nm wide permalloy nanowires with a small edge-to-edge separation of 45 nm. Provoking antiparallel alignment of the magnetization of neighboring nanowires, we unexpectedly find reciprocal excitation of Damon-Eshbach type SWs. The characteristics are in contrast to ferromagnetic thin films and controlled via, both, the external magnetic field and magnetic states. The observed reciprocal excitation is a metamaterial property for SWs and attributed to the peculiar magnetic symmetry of the artificially tailored magnetic material. The findings offer great perspectives for nanoscale SW interference devices. © 2013 American Institute of Physics. [http://dx.doi.org/10.1063/1.4773522]

Spectroscopy performed on periodic arrays of bistable ferromagnetic nanowires has evidenced magnonic crystal (MC) behavior reflecting a man-made band structure for spin waves (SWs).[1,2] Periodic nanowires of identical width have recently been shown to form a special class of artificial crystal offering unprecedented functionality via reprogrammed band structures. Different magnetic states such as ferromagnetic order (FMO) and antiferromagnetic order (AFO) allowed one to redefine the unit cell and periodicity of the lattice in one-and-the-same one-dimensional (1D) MC.[3] At the same time, thin films and magnonic waveguides from yttrium iron garnet and $Ni_{80}Fe_{20}$ have been shown to exhibit non-reciprocal SW characteristics when Damon-Eshbach-type (DE) spin waves were excited by microwave antenna.[4–8] For DE modes, the wave vector **k** is perpendicular to the magnetization **M**. Spin waves travelling in opposite directions had markedly different precessional amplitudes. For MCs, this issue has not yet been addressed in detail[9,10] though reciprocity is of special interest for magneto-photonics[11] and advanced applications, such as reprogrammable filters and logic devices based on SWs.[12,13] Devices exploiting the interference of counterpropagating spin waves might be ineffective if SWs behave in a non-reciprocal manner. Control of the so-called non-reciprocity parameter β (Ref. 4) is therefore a key for magnonic applications.

In this paper, we report SWs transmitted through a 1D array of bistable permalloy ($Ni_{80}Fe_{20}$) nanowires [Fig. 1(a)] which are excited by a coplanar waveguide (CPW) antenna. We study, in particular, the so-called reprogrammable MC.[3] This MC allows us to measure group velocities v_g and non-reciprocity parameter β of DE SWs traveling in positive and negative x direction for, both, FMO and AFO states. The plane wave method (PWM)[14,15] is used to remodel quantitatively the eigenfrequencies and group velocities. In the FMO state, we observe the non-reciprocal behavior of DE-type modes as known from natural ferromagnetic materials. In the AFO state, unexpectedly, we find reciprocal SW excitation.

We explain this behavior considering the distinct magnetic symmetry of the artificial crystal, provoking a metamaterial property not found for the natural material. Our findings are
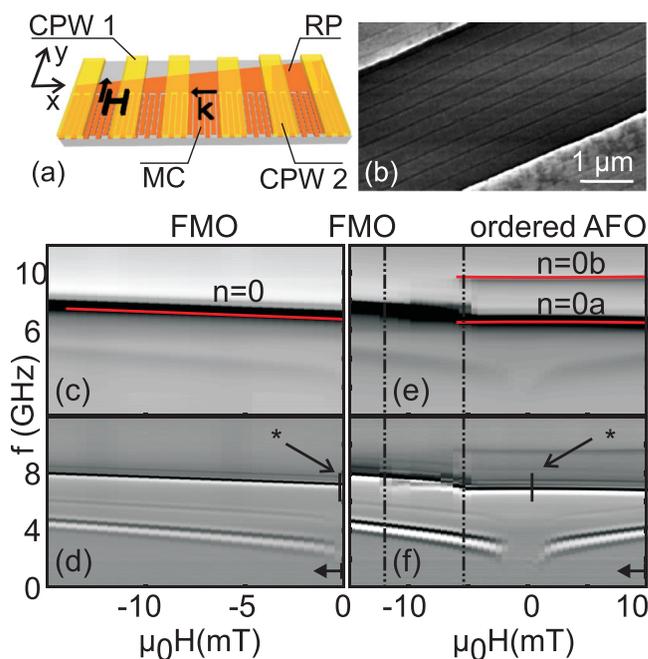

FIG. 1. (a) Sketch of emitter (CPW 1) and detector (CPW 2) CPWs on top of a nanowire array subject to a magnetic field **H**. **k** illustrates the transferred wave vector. Every second wire is connected to a RP. The z direction points out of the plane. (b) Scanning electron microscopy image of 255 nm wide wires with an edge-to-edge separation of 45 nm. The bright areas are the ground lines of CPW 1 and CPW 2. (c) $\Im m(a_{11})$ and (d) $\Im m(a_{21})$ in the FMO state taken for decreasing H in a ML starting at $\mu_0 H_{ML} = 0$ mT after saturation at -100 mT. The FMO mode $n = 0$ calculated by PWM (line) is labeled. (e) $\Im m(a_{11})$ and (f) $\Im m(a_{21})$ in the AFO state taken for decreasing H starting at $\mu_0 H_{ML} = 10$ mT after saturation at -100 mT. The AFO modes $n = 0a$ and $n = 0b$ calculated by PWM (lines) are labeled. The dashed-dotted perpendicular lines separate three different magnetic states (from the right): AFO state, disordered state, and FMO state. The perpendicular lines (highlighted by an asterisk) in (d) and (f) indicate the position of spectra presented in Fig. 3. The low frequency mode $f < 5$ GHz in (d) and (f) corresponds to the RP. Horizontal arrows indicate the sweep direction of H.

a)grundler@ph.tum.de.

promising for the coherent control of SWs using nanopatterned MCs.

We prepared different closely packed nanowire arrays on GaAs substrates using electron-beam lithography, evaporation of 30 ± 2 nm thick permalloy ($Ni_{80}Fe_{20}$), and subsequent lift-off processing. Two neighboring CPWs are integrated on top of an insulating layer to explore SW propagation [Figs. 1(a) and 1(b)].[15–17] Here, we discuss results obtained on a 1D MC with a period $p = 300$ nm and an edge-to-edge separation d of 45 nm. The wires have a length of $l = 300\,\mu$m to significantly reduce magnetostatic interaction reported in Ref. 18. Every second nanowire is intentionally connected to about $5\,\mu$m wide permalloy stripe acting as a reversal pad (RP). Thereby, we follow the work of Topp *et al.*[19] in which the RP shifts the switching field distribution of every second nanowire to a smaller absolute value.[26] This shift allows us to enhance the degree of ordering in the AFO state, i.e., the antiparallel magnetic alignment of neighboring nanowires, as was shown in Ref. 19. Subsequently, a 5 nm thick Al_2O_3 layer was grown by atomic layer deposition to ensure electrical isolation. On top, two shortened CPWs are integrated by optical lithography and lift-off processing. Each line of a CPW has a width of $2\,\mu$m and the edge-to-edge separation between the lines is $1.6\,\mu$m. The distance between the centers of the CPWs is $s = 12\,\mu$m. The CPWs extend over the MC and RP. We perform experiments in the frequency domain by a 2-port vector network analyzer, where we measure scattering parameters S_{ij} ($i, j = 1, 2$ label the CPWs 1 and 2). A vector magnet provides in-plane fields $\mu_0 H$ of up to 100 mT. We take reference data sets $S_{ij}(\text{Ref})$ which we subtract from the raw data to extract the magnetic response $a_{ij} = S_{ij}(H) - S_{ij}(\text{Ref})$. $\mathfrak{Im}(a_{ij})$ is the imaginary part of a_{ij}. The quantity a_{ij} reflects the susceptibility. We use gray-scale plots to present our data. For $i = j$ ($i \neq j$), black (oscillating black-white-black) contrast represents a spin wave resonance (propagating spin wave). Importantly, the most prominent mode excited by the CPW exhibits a wavelength $\lambda = 2\pi/k_{\text{CPW}} \approx (2\pi/0.5)\,\mu$m $= 12.6\,\mu$m, extending over 42 nanowires. k_{CPW} is extracted from the Fourier analysis of the CPW's rf magnetic field.[20] Later, we will thus address the long wavelength limit, i.e., the metamaterial properties of the MC.[15] Experimental data will be compared to PWM calculations.[14,15] For this, we assume fully ordered ferro- and antiferromagnetic states where the dynamic magnetization $\mathbf{m}(x, t)$ obeys a lattice periodic function $\mathbf{m}'(x)$ in x direction [cf. Fig. 1(a)]. Propagating spin waves are described by a Bloch ansatz $\mathbf{m}(x, t) = \mathbf{m}'(x, t)\exp(i(kx - \omega t))$ where $\omega = 2\pi f$ (t) is the frequency (time). The underlying Landau-Lifshitz equation contains the relevant magnetostatic and dynamic coupling fields. Parameters are $M_S = 820$ kA/m, exchange constant $A = 1.0 \times 10^{-11}$ J/m, thickness of 28 nm, and out-of-plane anisotropy $K_u = 11.0 \times 10^{-4}$ J/m^2 as determined from ferromagnetic resonance performed on a series of reference thin films.

In Fig. 1(c), we depict $\mathfrak{Im}(a_{11})$ with H applied along the long axis of the nanowires. The sample is first saturated at $\mu_0 H_{\text{sat}} = -100$ mT. Then we apply $\mu_0 H_{\text{ML}} = 0$ mT and measure for decreasing H. In this minor loop (ML) measurement, $\mu_0 H_{\text{ML}} = 0$ mT is chosen such that the nanowires remain saturated in negative y direction. The eigenfrequency (dark) increases with decreasing H. This is the characteristic

behavior of the mode $n = 0$ in the FMO state[21] (n counts the number of nodal lines in a nanowire[22]). The branch in Fig. 1(c) is continuous (no kinks). Its slope is negative and uniform between $\mu_0 H = -15$ and 0 mT. The array is magnetically ordered in the FMO state in that the magnetization $\mathbf{M}_{\text{nw}}$ of each single nanowire is parallel to the neighboring one. In Fig. 1(d), the transmitted signal $\mathfrak{Im}(a_{21})$ is shown, taken for the same magnetic history and field regime. For a fixed H, the branch $n = 0$ exhibits an oscillatory black-white-black contrast as a function of f. Following Refs. 16 and 20, we attribute this signal to SWs propagating between emitter and detector CPWs with a velocity of a few km/s as will be quantified later. We will not discuss the resonances below 5 GHz that we attribute to the RP.

In the following, we discuss the 1D MC data, where the magnetic history induced the reversal of selected nanowires.[3,23] In Fig. 1(e), $\mathfrak{Im}(a_{11})$ is presented where the starting field $\mu_0 H_{\text{ML}} = +10$ mT is chosen such that half of the nanowires are expected to be reversed with respect to the initially saturated state at -100 mT. By this magnetic history, we follow Refs. 3, 23, and 24 to stabilize the AFO state. The branches are now subdivided in three regimes as was observed in Refs. 3 and 24. For -6 mT $< \mu_0 H < +10$ mT, we observe a prominent branch $n = 0a$ (black) near 6.5 GHz which exhibits a different slope compared to the branch $n = 0$ found for the FMO state of the same device in Fig. 1(c). The branch $n = 0a$ of negative curvature was recently attributed to the AFO state.[3] For -13 mT $< \mu_0 H < -6$ mT, we observe stepwise changes (kinks) in the resonance frequency reflecting the reversal of individual nanowires becoming realigned with the negative field direction. For $\mu_0 H < -13$ mT, the FMO branch $n = 0$ of Fig. 1(c) is recovered. Note that the quality of the spectra is such that we observe both the acoustic ($n = 0a$) and optical ($n = 0b$) branches of the AFO state between -6 and $+10$ mT. We also find the higher order mode with $n = 2$ (not shown). There is no signature of a remaining FMO mode in Fig. 1(e), and we obtain a spectrum a_{22} at CPW 2 (not shown) which is similar to a_{11} at CPW 1. These features substantiate an improved homogeneity of the AFO state compared to Refs. 3 and 18. In Fig. 1(f), the transmitted signal $\mathfrak{Im}(a_{21})$ is shown for the AFO state. The branch $n = 0a$ is near 6.5 GHz and supports propagating spin waves between -6 and $+10$ mT. The PWM quantitatively remodels the modes and field dependencies assuming a fully ordered AFO state [lines in Fig. 1(e)], i.e., a periodic lattice exhibiting a unit cell of two nanowires with anti-parallel $\mathbf{M}_{\text{nw}}$. We note that a fully periodic antiparallel alignment suggests a vector of the total magnetization $\mathbf{M}_{\text{tot}} = \sum \mathbf{M}_{\text{nw}} = 0$. Instead, $\mathbf{M}_{\text{tot}} = \mathbf{M}_S$ is valid for the FMO state.

In the following, we discuss the signal strength and reciprocity of counterpropagating SWs in FMO and AFO states. For this, we consider the propagation attenuation $\frac{a_{21}}{a_{11}}$ of SWs with wave vector k_{21} propagating from CPW 1 to CPW 2, and $\frac{a_{12}}{a_{22}}$ of SWs with k_{12} from CPW 2 to CPW 1 in Fig. 2(a).[16] In the FMO state with $\mathbf{M}_{\text{nw}}$ pointing in negative y direction, $\frac{a_{21}}{a_{11}} \left(\frac{a_{12}}{a_{22}}\right)$ varies with H between 0.06 and 0.07 (0.042 and 0.04). The FMO state with $\mathbf{M}_{\text{nw}}$ pointing in positive y direction exhibits values $\frac{a_{21}}{a_{11}} \left(\frac{a_{12}}{a_{22}}\right)$ of about 0.03 (0.07).
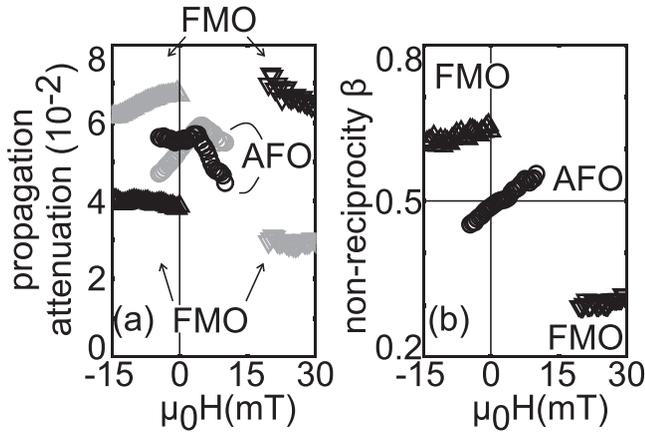
FIG. 2. (a) Propagation attenuation for counter-propagating SWs: $\frac{a_{21}}{a_{11}}$ (black) and $\frac{a_{12}}{a_{22}}$ (gray) (FMO with $\mu_0 H_{\mathrm{sat}} = -100$ mT: upward triangle, FMO with $\mu_0 H_{\mathrm{sat}} = 100$ mT: downward triangle, AFO: circle). (b) Non-reciprocity parameter β. FMO with $\mu_0 H_{\mathrm{sat}} = -100$ mT: upward triangle, FMO with $\mu_0 H_{\mathrm{sat}} = 100$ mT: downward triangle, AFO: circle. $\beta = 0.5$ indicates reciprocal excitation and is achieved in the AFO state. The field step is $\Delta \mu_0 H = 0.5$ mT.
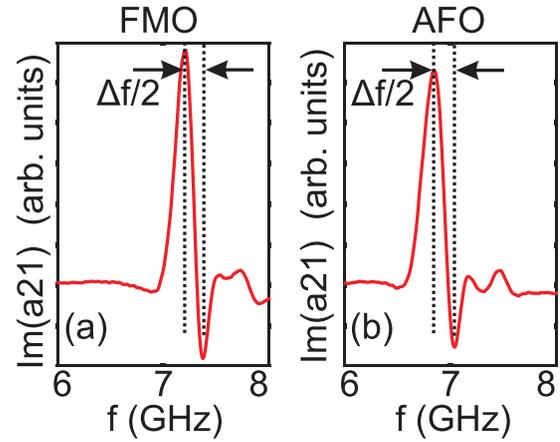

FIG. 3. (a) $\mathfrak{Im}(a_{21})$ for the FMO state at $\mu_0 H = 0$ mT. (b) $\mathfrak{Im}(a_{21})$ for the AFO state at $\mu_0 H = 2$ mT. The perpendicular dotted lines indicate $\Delta f/2$ between local extrema generated by phase shifts from propagating SWs.

The propagation attenuation of counterpropagating SWs differs thus considerably. By reversing $\mathbf{M}_{\mathrm{nw}}$, the propagation attenuation is found to nearly interchange. Importantly, in the AFO state, we observe a different behavior and obtain $\frac{a_{21}}{a_{11}} = \frac{a_{12}}{a_{22}}$ at $\mu_0 H = 2$ mT. Spin waves with k_{21} and k_{12} exhibit the same spin-precessional amplitudes at the relevant detector. Such a reciprocal behavior of DE modes is in contrast to Refs. 4 and 6. We define and evaluate the non-reciprocity parameter β using

$$a_{21} = \beta a_{11} \exp(-s/s_{\mathrm{r}})$$
$$a_{12} = (1 - \beta) a_{22} \exp(-s/s_{\mathrm{r}})$$
$$\Rightarrow \beta = \frac{\dfrac{a_{21}}{a_{11}}}{\dfrac{a_{21}}{a_{11}} + \dfrac{a_{12}}{a_{22}}}, \qquad (1)$$

where s_{r} is the relevant decay length in a given magnetic state which is the same for counter-propagating spin waves. $\beta = 0.5$ indicates reciprocal characteristics. For FMO, Eq. (1) yields $\beta_{\mathrm{FMO}} = 0.7$ for negative saturation and $\beta_{\mathrm{FMO}} = 0.3$ for positive saturation [Fig. 2(b)], i.e., $\beta \neq 0.5$ consistent with Refs. 4 and 6. For AFO, however, $\beta_{\mathrm{AFO}} = 0.5$ at $\mu_0 H = 2$ mT. For both increasing and decreasing H, β is found to deviate from 0.5. But values of β are still different from FMO data.

The non-reciprocal behavior for the FMO state can be explained following Demidov *et al.*,[4] who investigated counter-propagating DE modes in a homogeneous material with $\mathbf{M}_{\mathrm{tot}} = \mathbf{M}_{\mathrm{S}}$. The modes exhibited non-reciprocal characteristics because of partly counteracting components h_x and h_z of the rf magnetic field of the emitter antenna. Both components h_x and h_z provide torque contributions for SW excitation but have opposite phase relations at the opposite sides of the antenna. For in-phase (out-of-phase) relation, the corresponding torques enhanced (reduced) the precessional amplitude for SWs propagating to one (the other) direction. For plain films, this antenna-induced non-reciprocity is expected to increase with decreasing $\mathbf{M}_{\mathrm{tot}} = \mathbf{M}_{\mathrm{S}}$. An artificially tailored material

with $\mathbf{M}_{\mathrm{tot}} = 0$ such as a 1D MC in the AFO state has not yet been addressed. We observe that, strikingly, the non-reciprocity vanishes under such a condition ($\beta = 0.5$). We attribute this peculiar observation in the AFO state to a balanced configuration, i.e., the internal field in each nanowire is the same and amounts to $H_{\mathrm{int}} = 0$.[21] Considering the long wavelength of the SWs ($\lambda \gg p$), an equal number of positively and negatively magnetized nanowires are excited such that in-phase and out-of-phase torques through h_x and h_z average out in the relevant unit cells of the MC. Excitation on both sides of the CPW becomes similar. The reciprocal behavior is thus a metamaterial property for SWs. For the ideal 1D MC, $H_{\mathrm{int}} = 0$ is valid for $H = 0$. For real 1D MCs, it was reported that residual stray fields needed to be considered and compensated via a small H.[3,18] Consistently, we observe $\beta = 0.5$ at $\mu_0 H = 2$ mT. For other H, the AFO state is not balanced and H_{int} is known to vary periodically throughout the MC.[21] Then, the excitation of the two nanowires in the unit cell is no longer fully symmetric.[19,21] Figure 2(b) shows that the non-reciprocity is recovered for such unbalanced AFO states, allowing for a precise field control of the artificially created reciprocal SW excitation.

In Figs. 3(a) and 3(b), we show transmission spectra $\mathfrak{Im}(a_{21})$ for the FMO and AFO state, respectively, to evaluate relevant group velocities $v_{\mathrm{g}} = \Delta f \times s$.[20] We obtain $v_{\mathrm{g}} = 4.0 \pm 0.3$ km/s in the FMO state and $v_{\mathrm{g}} = 4.3 \pm 0.3$ km/s in the AFO state. The group velocities are found to differ by 8%. This experimental finding is supported by PWM that predicts 4%. This difference reflects the reprogrammed band structures. The absolute values obtained by PWM amount to $v_{\mathrm{g,FMO}} = 3.4$ km/s and $v_{\mathrm{g,AFO}} = 3.5$ km/s. We attribute the remaining discrepancy to edge roughness of the nanowires, which is not included in PWM and varies the dipolar interaction. It is instructive to compare these values with an intrinsically reciprocal magnetostatic forward volume wave (MSFVW) and magnetostatic backward volume wave (MSBVW). v_{g} for MSFVW (MSBVW) in a permalloy thin film with similar parameters as used in this work is calculated to be 1.3 km/s (0.16 km/s). Strikingly, the 1D MC supports reciprocal SWs with v_{g} being larger by a factor of 3 (27). We thus consider the balanced AFO as an optimum

state for a thin-film spin wave bus, where fast propagation is desired with equal amplitudes in opposite directions.[25]

In conclusion, we studied spin wave propagation in 1D MCs with a reprogrammable band structure. The absolute frequencies as well as the group velocities are modeled by PWM calculations for FMO and AFO. The non-reciprocity parameter β is found to be 0.5 for AFO near $H = 0$. The reciprocal SW excitation is promising for coherent control on the nanoscale and for devices where counterpropagating DE modes are manipulated, e.g., in a SW interferometer device.

[1]M. P. Kostylev, A. A. Stashkevich, and N. A. Sergeeva, Phys. Rev. B **69**, 064408 (2004).
[2]G. Gubbiotti, S. Tacchi, G. Carlotti, P. Vavassori, N. Singh, S. Goolaup, A. O. Adeyeye, A. Stashkevich, and M. Kostylev, Phys. Rev. B **72**, 224413 (2005).
[3]J. Topp, D. Heitmann, M. P. Kostylev, and D. Grundler, Phys. Rev. Lett. **104**, 207205 (2010).
[4]V. E. Demidov, M. P. Kostylev, K. Rott, P. Krzysteczko, G. Reiss, and S. O. Demokritov, Appl. Phys. Lett. **95**, 112509 (2009).
[5]K. Sekiguchi, K. Yamada, S. M. Seo, K. J. Lee, D. Chiba, K. Kobayashi, and T. Ono, Appl. Phys. Lett. **97**, 022508 (2010).
[6]L. Fallarino, M. Madami, G. Duerr, D. Grundler, G. Gubbiotti, S. Tacchi, and G. Carlotti, "Propagation of spin waves excited in a Permalloy film by a finite-ground coplanar waveguide: a combined phase-sensitive micro-focused Brillouin light scattering and micromagnetic study," IEEE Trans. Magn. (in press).
[7]T. Schneider, A. A. Serga, T. Neumann, B. Hillebrands, and M. P. Kostylev, Phys. Rev. B **77**, 214411 (2008).
[8]O. Büttner, M. Bauer, S. O. Demokritov, B. Hillebrands, Y. S. Kivshar, V. Grimalsky, Y. Rapoport, and A. N. Slavin, Phys. Rev. B **61**, 11576 (2000).
[9]S. L. Vysotski, S. A. Nikitov, and Y. A. Filimonov, J. Exp. Theor. Phys. **101**, 547 (2005).
[10]A. A. Serga, A. V. Chumak, and B. Hillebrands, J. Phys. D: Appl. Phys. **43**, 264002 (2010).
[11]M. Inoue, R. Fujikawa, A. Baryshev, A. Khanikaev, P. B. Lim, H. Uchida, O. Aktsipetrov, A. Fedyanin, T. Murzina, and A. Granovsky, J. Phys. D: Appl. Phys. **39**, R151 (2006).
[12]S. Neusser and D. Grundler, Adv. Mater. **21**, 2927 (2009).
[13]A. Khitun, M. Bao, and K. L. Wang, J. Phys. D: Appl. Phys. **43**, 264005 (2010).
[14]M. Sokolovskyy and M. Krawczyk, J. Nanopart. Res. **13**, 6085 (2011).
[15]S. Neusser, H. G. Bauer, G. Duerr, R. Huber, S. Mamica, G. Woltersdorf, M. Krawczyk, C. H. Back, and D. Grundler, Phys. Rev. B **84**, 184411 (2011).
[16]M. Bailleul, D. Olligs, and C. Fermon, Appl. Phys. Lett. **83**, 972 (2003).
[17]M. Bao, K. Wong, A. Khitun, J. Lee, Z. Hao, K. L. Wang, D. W. Lee, and S. X. Wang, Europhys. Lett. **84**, 27009 (2008).
[18]J. Ding, M. Kostylev, and A. O. Adeyeye, Phys. Rev. B **84**, 054425 (2011).
[19]J. Topp, S. Mendach, D. Heitmann, M. Kostylev, and D. Grundler, Phys. Rev. B **84**, 214413 (2011).
[20]V. Vlaminck and M. Bailleul, Phys. Rev. B **81**, 014425 (2010).
[21]J. Topp, G. Duerr, K. Thurner, and D. Grundler, Pure Appl. Chem. **83**, 1989 (2011).
[22]M. P. Kostylev and A. A. Stashkevich, Phys. Rev. B **81**, 054418 (2010).
[23]S. Tacchi, M. Madami, G. Gubbiotti, G. Carlotti, S. Goolaup, A. O. Adeyeye, N. Singh, and M. P. Kostylev, Phys. Rev. B **82**, 184408 (2010).
[24]J. Ding, M. Kostylev, and A. O. Adeyeye, Phys. Rev. Lett. **107**, 047205 (2011).
[25]A. Khitun and K. L. Wang, Superlattices Microstruct. **38**, 184 (2005).
[26]We performed magnetic force microscopy (MFM) on a comparable MC incorporating a RP. The switching field distribution was found to shift to smaller absolute values. The MC discussed in this paper was not available for MFM.